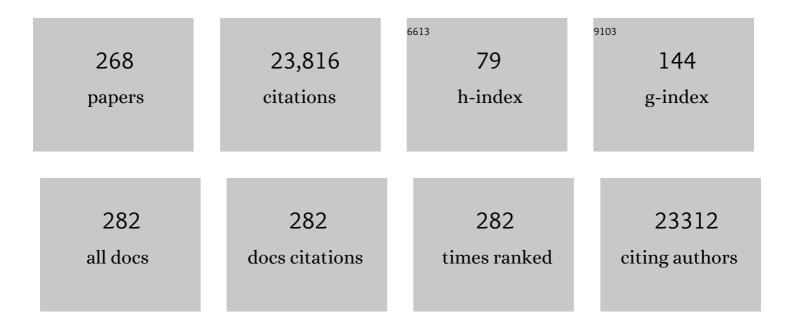
Gerhard Wagner

List of Publications by Year in descending order

Source: https://exaly.com/author-pdf/3383651/publications.pdf Version: 2024-02-01



#	Article	lF	CITATIONS
1	High fidelity sampling schedules for NMR spectra of high dynamic range. Journal of Magnetic Resonance, 2022, 339, 107228.	2.1	4
2	Pre–T cell receptors topologically sample self-ligands during thymocyte β-selection. Science, 2021, 371, 181-185.	12.6	25
3	Allosterically Coupled Multisite Binding of Testosterone to Human Serum Albumin. Endocrinology, 2021, 162, .	2.8	14
4	A multi-pronged approach targeting SARS-CoV-2 proteins using ultra-large virtual screening. IScience, 2021, 24, 102021.	4.1	66
5	Cryo-EM structure of an activated GPCR–G protein complex in lipid nanodiscs. Nature Structural and Molecular Biology, 2021, 28, 258-267.	8.2	71
6	Structural basis of the dynamic human CEACAM1 monomer-dimer equilibrium. Communications Biology, 2021, 4, 360.	4.4	6
7	VirtualFlow Ants—Ultra-Large Virtual Screenings with Artificial Intelligence Driven Docking Algorithm Based on Ant Colony Optimization. International Journal of Molecular Sciences, 2021, 22, 5807.	4.1	16
8	A biphenyl inhibitor of eIF4E targeting an internal binding site enables the design of cell-permeable PROTAC-degraders. European Journal of Medicinal Chemistry, 2021, 219, 113435.	5.5	15
9	Deep computational analysis details dysregulation of eukaryotic translation initiation complex elF4F in human cancers. Cell Systems, 2021, 12, 907-923.e6.	6.2	11
10	A general chemical crosslinking strategy for structural analyses of weakly interacting proteins applied to preTCR–pMHC complexes. Journal of Biological Chemistry, 2021, 296, 100255.	3.4	4
11	NUScon: a community-driven platform for quantitative evaluation of nonuniform sampling in NMR. Magnetic Resonance, 2021, 2, 843-861.	1.9	7
12	The Structural Basis for Low Conductance in the Membrane Protein VDAC upon β-NADH Binding and Voltage Gating. Structure, 2020, 28, 206-214.e4.	3.3	28
13	Conformational gating, dynamics and allostery in human monoacylglycerol lipase. Scientific Reports, 2020, 10, 18531.	3.3	8
14	Modulating TRADD to restore cellular homeostasis and inhibit apoptosis. Nature, 2020, 587, 133-138.	27.8	57
15	Nearest-neighbor NMR spectroscopy: categorizing spectral peaks by their adjacent nuclei. Nature Communications, 2020, 11, 5547.	12.8	10
16	Large Nanodiscs: A Potential Game Changer in Structural Biology of Membrane Protein Complexes and Virus Entry. Frontiers in Bioengineering and Biotechnology, 2020, 8, 539.	4.1	17
17	The precious fluorine on the ring: fluorine NMR for biological systems. Journal of Biomolecular NMR, 2020, 74, 365-379.	2.8	31
18	An open-source drug discovery platform enables ultra-large virtual screens. Nature, 2020, 580, 663-668.	27.8	345

#	Article	IF	CITATIONS
19	A newly identified Leishmania IF4E-interacting protein, Leish4E-IP2, modulates the activity of cap-binding protein paralogs. Nucleic Acids Research, 2020, 48, 4405-4417.	14.5	10
20	Accounting of Receptor Flexibility in Ultra-Large Virtual Screens with VirtualFlow Using a Grey Wolf Optimization Method. Supercomputing Frontiers and Innovations, 2020, 7, 4-12.	0.4	7
21	Discovery of small-molecule inhibitors targeting the ribosomal peptidyl transferase center (PTC) of <i>M. tuberculosis</i> . Chemical Science, 2019, 10, 8764-8767.	7.4	10
22	Integrative methods in structural biology. Journal of Biomolecular NMR, 2019, 73, 261-263.	2.8	7
23	Emerging solution NMR methods to illuminate the structural and dynamic properties of proteins. Current Opinion in Structural Biology, 2019, 58, 294-304.	5.7	26
24	Topological analysis of the gp41 MPER on lipid bilayers relevant to the metastable HIV-1 envelope prefusion state. Proceedings of the National Academy of Sciences of the United States of America, 2019, 116, 22556-22566.	7.1	22
25	Structural characterization of the human membrane protein VDAC2 in lipid bilayers by MAS NMR. Journal of Biomolecular NMR, 2019, 73, 451-460.	2.8	13
26	A nanobody that recognizes a 14-residue peptide epitope in the E2 ubiquitin-conjugating enzyme UBC6e modulates its activity. Molecular Immunology, 2019, 114, 513-523.	2.2	36
27	Aromatic 19F-13C TROSY: a background-free approach to probe biomolecular structure, function, and dynamics. Nature Methods, 2019, 16, 333-340.	19.0	82
28	NMR: an essential structural tool for integrative studies of T cell development, pMHC ligand recognition and TCR mechanobiology. Journal of Biomolecular NMR, 2019, 73, 319-332.	2.8	18
29	Nonuniform Sampling for NMR Spectroscopy. Methods in Enzymology, 2019, 614, 263-291.	1.0	31
30	¹⁵ N detection harnesses the slow relaxation property of nitrogen: Delivering enhanced resolution for intrinsically disordered proteins. Proceedings of the National Academy of Sciences of the United States of America, 2018, 115, E1710-E1719.	7.1	40
31	Mixed pyruvate labeling enables backbone resonance assignment of large proteins using a single experiment. Nature Communications, 2018, 9, 356.	12.8	13
32	Cytocapsular tubes conduct cell translocation. Proceedings of the National Academy of Sciences of the United States of America, 2018, 115, E1137-E1146.	7.1	9
33	Recent developments in solution nuclear magnetic resonance (NMR)-based molecular biology. Journal of Molecular Medicine, 2018, 96, 1-8.	3.9	23
34	Covalently circularized nanodiscs; challenges and applications. Current Opinion in Structural Biology, 2018, 51, 129-134.	5.7	31
35	Structural basis for LeishIF4E-1 modulation by an interacting protein in the human parasite Leishmania major. Nucleic Acids Research, 2018, 46, 3791-3801.	14.5	19
36	Assembly of phospholipid nanodiscs of controlled size for structural studies of membrane proteins by NMR. Nature Protocols, 2018, 13, 79-98.	12.0	159

#	Article	IF	CITATIONS
37	NMR-directed design of pre-TCRÎ ² and pMHC molecules implies a distinct geometry for pre-TCR relative to αβTCR recognition of pMHC. Journal of Biological Chemistry, 2018, 293, 754-766.	3.4	14
38	High resolution X-ray and NMR structural study of human T-cell immunoglobulin and mucin domain containing protein-3. Scientific Reports, 2018, 8, 17512.	3.3	35
39	Cytidine monophosphate N -acetylneuraminic acid synthetase enhances invasion of human triple-negative breast cancer cells. OncoTargets and Therapy, 2018, Volume 11, 6827-6838.	2.0	8
40	The T Cell Antigen Receptor α Transmembrane Domain Coordinates Triggering through Regulation of Bilayer Immersion and CD3 Subunit Associations. Immunity, 2018, 49, 829-841.e6.	14.3	58
41	Optimal control theory enables homonuclear decoupling without Bloch–Siegert shifts in NMR spectroscopy. Nature Communications, 2018, 9, 3014.	12.8	26
42	DNA-Corralled Nanodiscs for the Structural and Functional Characterization of Membrane Proteins and Viral Entry. Journal of the American Chemical Society, 2018, 140, 10639-10643.	13.7	57
43	Rapid convergence of optimal control in NMR using numerically-constructed toggling frames. Journal of Magnetic Resonance, 2017, 281, 94-103.	2.1	12
44	1H, 13C, and 15N backbone chemical shift assignments of 4E-BP144–87 and 4E-BP144–87 bound to elF4E. Biomolecular NMR Assignments, 2017, 11, 187-191.	0.8	1
45	Interpolating and extrapolating with hmsIST:Âseeking a tmax for optimal sensitivity, resolution and frequency accuracy. Journal of Biomolecular NMR, 2017, 68, 139-154.	2.8	24
46	Molecular Landscape of the Ribosome Pre-initiation Complex during mRNA Scanning: Structural Role for eIF3c and Its Control by eIF5. Cell Reports, 2017, 18, 2651-2663.	6.4	54
47	Covalently circularized nanodiscs for studying membrane proteins and viral entry. Nature Methods, 2017, 14, 49-52.	19.0	221
48	Solution Structure of the Cuz1 AN1 Zinc Finger Domain: An Exposed LDFLP Motif Defines a Subfamily of AN1 Proteins. PLoS ONE, 2016, 11, e0163660.	2.5	3
49	The Role of Dynamics and Allostery in the Inhibition of the eIF4E/eIF4G Translation Initiation Factor Complex. Angewandte Chemie, 2016, 128, 7292-7295.	2.0	1
50	The Role of Dynamics and Allostery in the Inhibition of the eIF4E/eIF4G Translation Initiation Factor Complex. Angewandte Chemie - International Edition, 2016, 55, 7176-7179.	13.8	14
51	Nitrogen-detected TROSY yields comparable sensitivity to proton-detected TROSY for non-deuterated, large proteins under physiological salt conditions. Journal of Biomolecular NMR, 2016, 64, 143-151.	2.8	34
52	Pre-T Cell Receptors (Pre-TCRs) Leverage VÎ ² Complementarity Determining Regions (CDRs) and Hydrophobic Patch in Mechanosensing Thymic Self-ligands. Journal of Biological Chemistry, 2016, 291, 25292-25305.	3.4	60
53	Analytical optimization of active bandwidth and quality factor for TOCSY experiments in NMR spectroscopy. Journal of Biomolecular NMR, 2016, 66, 9-20.	2.8	5
54	An accurately preorganized IRES RNA structure enables eIF4G capture for initiation of viral translation. Nature Structural and Molecular Biology, 2016, 23, 859-864.	8.2	42

#	Article	IF	CITATIONS
55	Perspective: revisiting the field dependence of TROSY sensitivity. Journal of Biomolecular NMR, 2016, 66, 221-225.	2.8	19
56	Identification of DNA primase inhibitors via a combined fragment-based and virtual screening. Scientific Reports, 2016, 6, 36322.	3.3	18
57	Overexpression of eIF5 or its protein mimic 5MP perturbs eIF2 function and induces <i>ATF4</i> translation through delayed re-initiation. Nucleic Acids Research, 2016, 44, 8704-8713.	14.5	40
58	Conformational dynamics of a C-protein α subunit is tightly regulated by nucleotide binding. Proceedings of the National Academy of Sciences of the United States of America, 2016, 113, E3629-38.	7.1	77
59	Inhibiting fungal multidrug resistance by disrupting an activator–Mediator interaction. Nature, 2016, 530, 485-489.	27.8	120
60	UTOPIA NMR: activating unexploited magnetization using interleaved low-gamma detection. Journal of Biomolecular NMR, 2016, 64, 9-15.	2.8	19
61	Backbone resonance assignment of N15, N30 and D10 T cell receptor β subunits. Biomolecular NMR Assignments, 2016, 10, 35-39.	0.8	4
62	<scp>NMR</scp> studies reveal a novel grab and release mechanism for efficient catalysis of the bacterial 2 ys peroxiredoxin machinery. FEBS Journal, 2015, 282, 4620-4638.	4.7	9
63	Structural Features of the \hat{l} + \hat{l}^2 TCR Mechanotransduction Apparatus That Promote pMHC Discrimination. Frontiers in Immunology, 2015, 6, 441.	4.8	55
64	An RNA-binding Protein, Lin28, Recognizes and Remodels G-quartets in the MicroRNAs (miRNAs) and mRNAs It Regulates. Journal of Biological Chemistry, 2015, 290, 17909-17922.	3.4	32
65	Pre-TCR ligand binding impacts thymocyte development before αβTCR expression. Proceedings of the National Academy of Sciences of the United States of America, 2015, 112, 8373-8378.	7.1	62
66	elF1A augments Ago2-mediated Dicer-independent miRNA biogenesis and RNA interference. Nature Communications, 2015, 6, 7194.	12.8	39
67	Nitrogen detected TROSY at high field yields high resolution and sensitivity for protein NMR. Journal of Biomolecular NMR, 2015, 63, 323-331.	2.8	40
68	Lipid bilayer-bound conformation of an integral membrane beta barrel protein by multidimensional MAS NMR. Journal of Biomolecular NMR, 2015, 61, 299-310.	2.8	38
69	Magic Angle Spinning Nuclear Magnetic Resonance Characterization of Voltage-Dependent Anion Channel Gating in Two-Dimensional Lipid Crystalline Bilayers. Biochemistry, 2015, 54, 994-1005.	2.5	34
70	Force-dependent transition in the T-cell receptor β-subunit allosterically regulates peptide discrimination and pMHC bond lifetime. Proceedings of the National Academy of Sciences of the United States of America, 2015, 112, 1517-1522.	7.1	209
71	Structure refinement and membrane positioning of selectively labeled OmpX in phospholipid nanodiscs. Journal of Biomolecular NMR, 2015, 61, 249-260.	2.8	48
72	NMR resonance assignments of the catalytic domain of human serine/threonine phosphatase calcineurin in unligated and PVIVIT-peptide-bound states. Biomolecular NMR Assignments, 2015, 9, 201-205.	0.8	5

#	Article	IF	CITATIONS
73	Increased resolution of aromatic cross peaks using alternate 13C labeling and TROSY. Journal of Biomolecular NMR, 2015, 62, 291-301.	2.8	26
74	Molecular mechanism of the dual activity of 4EGI-1: Dissociating eIF4G from eIF4E but stabilizing the binding of unphosphorylated 4E-BP1. Proceedings of the National Academy of Sciences of the United States of America, 2015, 112, E4036-45.	7.1	90
75	Structure of a herpesvirus nuclear egress complex subunit reveals an interaction groove that is essential for viral replication. Proceedings of the National Academy of Sciences of the United States of America, 2015, 112, 9010-9015.	7.1	52
76	NMR studies of membrane proteins. Journal of Biomolecular NMR, 2015, 61, 181-184.	2.8	6
77	The membrane anchor of the transcriptional activator SREBP is characterized by intrinsic conformational flexibility. Proceedings of the National Academy of Sciences of the United States of America, 2015, 112, 12390-12395.	7.1	14
78	Controlled Co-reconstitution of Multiple Membrane Proteins in Lipid Bilayer Nanodiscs Using DNA as a Scaffold. ACS Chemical Biology, 2015, 10, 2448-2454.	3.4	21
79	Structure of a CGI-58 Motif Provides the Molecular Basis of Lipid Droplet Anchoring. Journal of Biological Chemistry, 2015, 290, 26361-26372.	3.4	43
80	1H, 13C, and 15N backbone and sidechain chemical shift assignments for the HEAT2 domain of human eIF4GI. Biomolecular NMR Assignments, 2015, 9, 157-160.	0.8	0
81	Essential role of elF5-mimic protein in animal development is linked to control of ATF4 expression. Nucleic Acids Research, 2014, 42, 10321-10330.	14.5	24
82	Molecular Signatures of Hemagglutinin Stem-Directed Heterosubtypic Human Neutralizing Antibodies against Influenza A Viruses. PLoS Pathogens, 2014, 10, e1004103.	4.7	121
83	A new broadband homonuclear mixing pulse for NMR with low applied power. Journal of Chemical Physics, 2014, 141, 024201.	3.0	6
84	Human Translation Initiation Factor elF4G1 Possesses a Low-Affinity ATP Binding Site Facing the ATP-Binding Cleft of elF4A in the elF4G/elF4A Complex. Biochemistry, 2014, 53, 6422-6425.	2.5	2
85	Backbone resonance assignment of the HEAT1-domain of the human eukaryotic translation initiation factor 4GI. Biomolecular NMR Assignments, 2014, 8, 89-91.	0.8	6
86	Disruption of Helix-Capping Residues 671 and 674 Reveals a Role in HIV-1 Entry for a Specialized Hinge Segment of the Membrane Proximal External Region of gp41. Journal of Molecular Biology, 2014, 426, 1095-1108.	4.2	34
87	G-quadruplex structures contribute to the neuroprotective effects of angiogenin-induced tRNA fragments. Proceedings of the National Academy of Sciences of the United States of America, 2014, 111, 18201-18206.	7.1	264
88	Examining weak protein–protein interactions in start codon recognition via <scp>NMR</scp> spectroscopy. FEBS Journal, 2014, 281, 1965-1973.	4.7	12
89	Structure of the eukaryotic translation initiation factor elF4E in complex with 4EGI-1 reveals an allosteric mechanism for dissociating elF4G. Proceedings of the National Academy of Sciences of the United States of America, 2014, 111, E3187-95.	7.1	72
90	Quantitative phosphoproteomic analysis reveals system-wide signaling pathways downstream of SDF-1/CXCR4 in breast cancer stem cells. Proceedings of the National Academy of Sciences of the United States of America, 2014, 111, E2182-90.	7.1	109

#	Article	IF	CITATIONS
91	Constitutively Oxidized CXXC Motifs within the CD3 Heterodimeric Ectodomains of the T Cell Receptor Complex Enforce the Conformation of Juxtaposed Segments. Journal of Biological Chemistry, 2014, 289, 18880-18892.	3.4	24
92	The LxVP and PxIxIT NFAT Motifs Bind Jointly to Overlapping Epitopes on Calcineurin's Catalytic Domain Distant to the Regulatory Domain. Structure, 2014, 22, 1016-1027.	3.3	15
93	Selective Methyl Labeling of Eukaryotic Membrane Proteins Using Cell-Free Expression. Journal of the American Chemical Society, 2014, 136, 11308-11310.	13.7	36
94	Solid-State NMR Structure Determination from Diagonal-Compensated, Sparsely Nonuniform-Sampled 4D Proton–Proton Restraints. Journal of the American Chemical Society, 2014, 136, 11002-11010.	13.7	61
95	Discovery and Characterization of a Disulfide-Locked <i>C</i> ₂ -Symmetric Defensin Peptide. Journal of the American Chemical Society, 2014, 136, 13494-13497.	13.7	50
96	Perspectives in magnetic resonance: NMR in the post-FFT era. Journal of Magnetic Resonance, 2014, 241, 60-73.	2.1	122
97	Structure–activity relationship study of 4EGI-1, small molecule eIF4E/eIF4G protein–protein interaction inhibitors. European Journal of Medicinal Chemistry, 2014, 77, 361-377.	5.5	18
98	The Use of Amphipols for NMR Structural Characterization of 7-TM Proteins. Journal of Membrane Biology, 2014, 247, 957-964.	2.1	26
99	Resonance assignments of the microtubule-binding domain of the C. elegans spindle and kinetochore-associated protein 1. Biomolecular NMR Assignments, 2014, 8, 275-278.	0.8	5
100	4EGI-1 targets breast cancer stem cells by selective inhibition of translation that persists in CSC maintenance, proliferation and metastasis. Oncotarget, 2014, 5, 6028-6037.	1.8	29
101	Cell-free Expressed Bacteriorhodopsin in Different Soluble Membrane Mimetics: Biophysical Properties and NMR Accessibility. Structure, 2013, 21, 394-401.	3.3	103
102	Immunogenicity of Membrane-bound HIV-1 gp41 Membrane-proximal External Region (MPER) Segments Is Dominated by Residue Accessibility and Modulated by Stereochemistry. Journal of Biological Chemistry, 2013, 288, 31888-31901.	3.4	43
103	Exploring new limits in complex biological structures. Current Opinion in Structural Biology, 2013, 23, 704-706.	5.7	2
104	Exploring signal-to-noise ratio and sensitivity in non-uniformly sampled multi-dimensional NMR spectra. Journal of Biomolecular NMR, 2013, 55, 167-178.	2.8	96
105	Pulse design for broadband correlation NMR spectroscopy by multi-rotating frames. Journal of Biomolecular NMR, 2013, 55, 291-302.	2.8	11
106	Optimized Phospholipid Bilayer Nanodiscs Facilitate High-Resolution Structure Determination of Membrane Proteins. Journal of the American Chemical Society, 2013, 135, 1919-1925.	13.7	445
107	Molecular Crowding Enhanced ATPase Activity of the RNA Helicase eIF4A Correlates with Compaction of Its Quaternary Structure and Association with eIF4G. Journal of the American Chemical Society, 2013, 135, 10040-10047.	13.7	35
108	The Interaction between Eukaryotic Initiation Factor 1A and eIF5 Retains eIF1 within Scanning Preinitiation Complexes. Biochemistry, 2013, 52, 9510-9518.	2.5	37

#	Article	IF	CITATIONS
109	β-Hairpin Loop of Eukaryotic Initiation Factor 1 (eIF1) Mediates 40 S Ribosome Binding to Regulate Initiator tRNAMet Recruitment and Accuracy of AUG Selection in Vivo. Journal of Biological Chemistry, 2013, 288, 27546-27562.	3.4	44
110	Hypoxia-inducible Factor-1α (HIF-1α) Promotes Cap-dependent Translation of Selective mRNAs through Up-regulating Initiation Factor eIF4E1 in Breast Cancer Cells under Hypoxia Conditions. Journal of Biological Chemistry, 2013, 288, 18732-18742.	3.4	55
111	Abstract 109: Preliminary Structural Into the Sterol Regulatory Element-Binding Protein (SREBP) Interaction With SREBP Cleavage-Activating Protein (SCAP). Arteriosclerosis, Thrombosis, and Vascular Biology, 2013, 33, .	2.4	0
112	Lipid Dynamics and Protein–Lipid Interactions in 2D Crystals Formed with the β-Barrel Integral Membrane Protein VDAC1. Journal of the American Chemical Society, 2012, 134, 6375-6387.	13.7	65
113	Solution NMR spectroscopic characterization of human VDAC-2 in detergent micelles and lipid bilayer nanodiscs. Biochimica Et Biophysica Acta - Biomembranes, 2012, 1818, 1562-1569.	2.6	53
114	The C-Terminal Domain of Eukaryotic Initiation Factor 5 Promotes Start Codon Recognition by Its Dynamic Interplay with eIF1 and eIF2β. Cell Reports, 2012, 1, 689-702.	6.4	66
115	The Kinetochore-Bound Ska1 Complex Tracks Depolymerizing Microtubules and Binds to Curved Protofilaments. Developmental Cell, 2012, 23, 968-980.	7.0	194
116	NMR Solution Structure and Condition-Dependent Oligomerization of the Antimicrobial Peptide Human Defensin 5. Biochemistry, 2012, 51, 9624-9637.	2.5	45
117	TCR Mechanobiology: Torques and Tunable Structures Linked to Early T Cell Signaling. Frontiers in Immunology, 2012, 3, 76.	4.8	75
118	Application of iterative soft thresholding for fast reconstruction of NMR data non-uniformly sampled with multidimensional Poisson Gap scheduling. Journal of Biomolecular NMR, 2012, 52, 315-327.	2.8	381
119	Editorial management of the Journal of Biomolecular NMR. Journal of Biomolecular NMR, 2012, 52, 3-4.	2.8	1
120	Tumor suppression by small molecule inhibitors of translation initiation. Oncotarget, 2012, 3, 869-881.	1.8	91
121	Applications of Non-Uniform Sampling and Processing. Topics in Current Chemistry, 2011, 316, 125-148.	4.0	119
122	Antibody mechanics on a membrane-bound HIV segment essential for GP41-targeted viral neutralization. Nature Structural and Molecular Biology, 2011, 18, 1235-1243.	8.2	86
123	Structure of the VP16 transactivator target in the Mediator. Nature Structural and Molecular Biology, 2011, 18, 410-415.	8.2	75
124	HNCA-TOCSY-CANH experiments with alternate 13C-12C labeling: a set of 3D experiment with unique supra-sequential information for mainchain resonance assignment. Journal of Biomolecular NMR, 2011, 49, 17-26.	2.8	10
125	Speeding up direct 15N detection: hCaN 2D NMR experiment. Journal of Biomolecular NMR, 2011, 51, 497-504.	2.8	23
126	Inhibition of the interactions between eukaryotic initiation factors 4E and 4G impairs long-term associative memory consolidation but not reconsolidation. Proceedings of the National Academy of Sciences of the United States of America, 2011, 108, 3383-3388.	7.1	95

#	Article	IF	CITATIONS
127	Molecular Characterization of Disrupted in Schizophrenia-1 Risk Variant S704C Reveals the Formation of Altered Oligomeric Assembly. Journal of Biological Chemistry, 2011, 286, 44266-44276.	3.4	26
128	A novel 4E-interacting protein in Leishmania is involved in stage-specific translation pathways. Nucleic Acids Research, 2011, 39, 8404-8415.	14.5	69
129	Transient Domain Interactions in Nonâ€Ribosomal Peptide Synthetases. FASEB Journal, 2011, 25, .	0.5	0
130	Backbone and ILV side chain methyl group assignments of the integral human membrane protein VDAC-1. Biomolecular NMR Assignments, 2010, 4, 29-32.	0.8	10
131	Overcoming the solubility limit with solubility-enhancement tags: successful applications in biomolecular NMR studies. Journal of Biomolecular NMR, 2010, 46, 23-31.	2.8	72
132	CACA-TOCSY with alternate 13C–12C labeling: a 13Cα direct detection experiment for mainchain resonance assignment, dihedral angle information, and amino acid type identification. Journal of Biomolecular NMR, 2010, 47, 55-63.	2.8	23
133	Nitrogen-detected CAN and CON experiments as alternative experiments for main chain NMR resonance assignments. Journal of Biomolecular NMR, 2010, 47, 271-282.	2.8	34
134	The 3D structures of VDAC represent a native conformation. Trends in Biochemical Sciences, 2010, 35, 514-521.	7.5	115
135	Distinctive CD3 Heterodimeric Ectodomain Topologies Maximize Antigen-Triggered Activation of αβ T Cell Receptors. Journal of Immunology, 2010, 185, 2951-2959.	0.8	34
136	Autoinhibitory Interaction in the Multidomain Adaptor Protein Nck: Possible Roles in Improving Specificity and Functional Diversity. Biochemistry, 2010, 49, 5634-5641.	2.5	11
137	Poisson-Gap Sampling and Forward Maximum Entropy Reconstruction for Enhancing the Resolution and Sensitivity of Protein NMR Data. Journal of the American Chemical Society, 2010, 132, 2145-2147.	13.7	308
138	High-Resolution 3D CANCA NMR Experiments for Complete Mainchain Assignments Using C ^α Direct Detection. Journal of the American Chemical Society, 2010, 132, 2945-2951.	13.7	25
139	Nonmicellar systems for solution NMR spectroscopy of membrane proteins. Current Opinion in Structural Biology, 2010, 20, 471-479.	5.7	114
140	Evidence for an Alternative Glycolytic Pathway in Rapidly Proliferating Cells. Science, 2010, 329, 1492-1499.	12.6	586
141	The αβ T Cell Receptor Is an Anisotropic Mechanosensor. Journal of Biological Chemistry, 2009, 284, 31028-31037.	3.4	350
142	Evolutionary changes in the Leishmania eIF4F complex involve variations in the eIF4E–eIF4G interactions. Nucleic Acids Research, 2009, 37, 3243-3253.	14.5	65
143	Coupled Decomposition of Four-Dimensional NOESY Spectra. Journal of the American Chemical Society, 2009, 131, 12970-12978.	13.7	51
144	Broadly neutralizing anti-HIV-1 antibodies disrupt a hinge-related function of gp41 at the membrane interface. Proceedings of the National Academy of Sciences of the United States of America, 2009, 106, 9057-9062.	7.1	104

#	Article	IF	CITATIONS
145	The role of solution NMR in the structure determinations of VDAC-1 and other membrane proteins. Current Opinion in Structural Biology, 2009, 19, 396-401.	5.7	81
146	The T-lock: automated compensation of radio-frequency induced sample heating. Journal of Biomolecular NMR, 2009, 44, 69-76.	2.8	6
147	FM reconstruction of non-uniformly sampled protein NMR data at higher dimensions and optimization by distillation. Journal of Biomolecular NMR, 2009, 45, 283-294.	2.8	69
148	Time-shared HSQC-NOESY for accurate distance constraints measured at high-field in 15N-13C-ILV methyl labeled proteins. Journal of Biomolecular NMR, 2009, 45, 311-318.	2.8	14
149	Topology and Regulation of the Human eIF4A/4G/4H Helicase Complex in Translation Initiation. Cell, 2009, 136, 447-460.	28.9	205
150	A Double TROSY hNCAnH Experiment for Efficient Assignment of Large and Challenging Proteins. Journal of the American Chemical Society, 2009, 131, 12880-12881.	13.7	23
151	Structural and Functional Characterization of the Integral Membrane Protein VDAC-1 in Lipid Bilayer Nanodiscs. Journal of the American Chemical Society, 2009, 131, 17777-17779.	13.7	158
152	A nuclear receptor-like pathway regulating multidrug resistance in fungi. Nature, 2008, 452, 604-609.	27.8	294
153	Structural basis for the selectivity of the external thioesterase of the surfactin synthetase. Nature, 2008, 454, 907-911.	27.8	112
154	Dynamic thiolation–thioesterase structure of a non-ribosomal peptide synthetase. Nature, 2008, 454, 903-906.	27.8	151
155	In situ observation of protein phosphorylation by high-resolution NMR spectroscopy. Nature Structural and Molecular Biology, 2008, 15, 321-329.	8.2	153
156	Identification of RIP1 kinase as a specific cellular target of necrostatins. Nature Chemical Biology, 2008, 4, 313-321.	8.0	1,708
157	Structural and Functional Evidence that Nck Interaction with CD3ε Regulates T-Cell Receptor Activity. Journal of Molecular Biology, 2008, 380, 704-716.	4.2	43
158	HIV-1 Broadly Neutralizing Antibody Extracts Its Epitope from a Kinked gp41 Ectodomain Region on the Viral Membrane. Immunity, 2008, 28, 52-63.	14.3	263
159	Solution Structure of the Integral Human Membrane Protein VDAC-1 in Detergent Micelles. Science, 2008, 321, 1206-1210.	12.6	605
160	Alternate ¹³ Câ^' ¹² C Labeling for Complete Mainchain Resonance Assignments using Cα Direct-Detection with Applicability Toward Fast Relaxing Protein Systems. Journal of the American Chemical Society, 2008, 130, 17210-17211.	13.7	42
161	Effects of Redox Potential and Ca2+ on the Inositol 1,4,5-Trisphosphate Receptor L3-1 Loop Region. Journal of Biological Chemistry, 2008, 283, 25567-25575.	3.4	39
162	Modern NMR in Undergraduate Education: Introduction. ACS Symposium Series, 2007, , 1-6.	0.5	0

#	Article	IF	CITATIONS
163	Molecular Framework for the Activation of RNA-dependent Protein Kinase. Journal of Biological Chemistry, 2007, 282, 11474-11486.	3.4	56
164	Importance of the CD3Î ³ Ectodomain Terminal Î ² -Strand and Membrane Proximal Stalk in Thymic Development and Receptor Assembly. Journal of Immunology, 2007, 178, 3668-3679.	0.8	22
165	Small-Molecule Inhibition of the Interaction between the Translation Initiation Factors eIF4E and eIF4G. Cell, 2007, 128, 257-267.	28.9	497
166	NMR Methods for Studying Protein–Protein Interactions Involved in Translation Initiation. Methods in Enzymology, 2007, 430, 283-331.	1.0	48
167	Ultrahigh-Resolution1Hâ~'13C HSQC Spectra of Metabolite Mixtures Using Nonlinear Sampling and Forward Maximum Entropy Reconstruction. Journal of the American Chemical Society, 2007, 129, 5108-5116.	13.7	131
168	NMR Structural Investigation of the Mitochondrial Outer Membrane Protein VDAC and Its Interaction with Antiapoptotic Bcl-xLâ€. Biochemistry, 2007, 46, 514-525.	2.5	148
169	Sequence and structure evolved separately in a ribosomal ubiquitin variant. EMBO Journal, 2007, 26, 3474-3483.	7.8	21
170	Structure of the Calcineurin-NFAT Complex: Defining a T Cell Activation Switch Using Solution NMR and Crystal Coordinates. Structure, 2007, 15, 587-597.	3.3	49
171	1-13C amino acid selective labeling in a 2H15N background for NMR studies of large proteins. Journal of Biomolecular NMR, 2007, 38, 89-98.	2.8	49
172	The role of crossâ€interface salt bridges in SCAN domain dimerization specificity. FASEB Journal, 2007, 21, A271.	0.5	0
173	Non-uniformly Sampled Double-TROSY hNcaNH Experiments for NMR Sequential Assignments of Large Proteins. Journal of the American Chemical Society, 2006, 128, 5757-5763.	13.7	63
174	NMR Distinction of Single- and Multiple-Mode Binding of Small-Molecule Protein Ligands. Journal of the American Chemical Society, 2006, 128, 2160-2161.	13.7	37
175	Mapping of the Auto-inhibitory Interactions of Protein Kinase R by Nuclear Magnetic Resonance. Journal of Molecular Biology, 2006, 364, 352-363.	4.2	35
176	An ARC/Mediator subunit required for SREBP control of cholesterol and lipid homeostasis. Nature, 2006, 442, 700-704.	27.8	351
177	Determination of all NOes in 1H–13C–Me-ILV-Uâ^'2H–15N Proteins with Two Time-Shared Experiments. Journal of Biomolecular NMR, 2006, 34, 31-40.	2.8	36
178	Solution Structure of the First Src Homology 3 Domain of Human Nck2. Journal of Biomolecular NMR, 2006, 34, 203-208.	2.8	14
179	Identification of individual protein–ligand NOEs in the limit of intermediate exchange. Journal of Biomolecular NMR, 2006, 36, 1-11.	2.8	23
180	NMR studies of protein interactions. Current Opinion in Structural Biology, 2006, 16, 109-117.	5.7	106

#	Article	IF	CITATIONS
181	Amplitudes and directions of internal protein motions from a JAM analysis of15N relaxation data. Magnetic Resonance in Chemistry, 2006, 44, S130-S142.	1.9	6
182	Structure of eukaryotic initiation factors at interfaces within ribosomal preinitiation complexes: Yeast perspectives. FASEB Journal, 2006, 20, A502.	0.5	0
183	Correspondence between spin-dynamic phases and pulse program phases of NMR spectrometers. Journal of Magnetic Resonance, 2005, 174, 325-330.	2.1	14
184	Fast Assignment of 15N-HSQC Peaks using High-Resolution 3D HNcocaNH Experiments with Non-Uniform Sampling. Journal of Biomolecular NMR, 2005, 33, 43-50.	2.8	59
185	Unambiguous Assignment of NMR Protein Backbone Signals with a Time-shared Triple-resonance Experiment. Journal of Biomolecular NMR, 2005, 33, 187-196.	2.8	31
186	High-resolution aliphatic side-chain assignments in 3D HCcoNH experiments with joint H–C evolution and non-uniform sampling. Journal of Biomolecular NMR, 2005, 32, 55-60.	2.8	29
187	Structural basis for the enhancement of eIF4A helicase activity by eIF4G. Genes and Development, 2005, 19, 2212-2223.	5.9	137
188	Mammalian SCAN Domain Dimer Is a Domain-Swapped Homolog of the HIV Capsid C-Terminal Domain. Molecular Cell, 2005, 17, 137-143.	9.7	81
189	Solution structure of the CD3ÂÂ ectodomain and comparison with CD3ÂÂ as a basis for modeling T cell receptor topology and signaling. Proceedings of the National Academy of Sciences of the United States of America, 2004, 101, 16867-16872.	7.1	101
190	Selective inhibition of calcineurin-NFAT signaling by blocking protein-protein interaction with small organic molecules. Proceedings of the National Academy of Sciences of the United States of America, 2004, 101, 7554-7559.	7.1	154
191	Accelerated acquisition of high resolution triple-resonance spectra using non-uniform sampling and maximum entropy reconstruction. Journal of Magnetic Resonance, 2004, 170, 15-21.	2.1	217
192	Discovery of Small-Molecule Inhibitors of the NFATâ^'Calcineurin Interaction by Competitive High-Throughput Fluorescence Polarization Screeningâ€. Biochemistry, 2004, 43, 16067-16075.	2.5	42
193	A General Framework for Development and Data Analysis of Competitive High-Throughput Screens for Small-Molecule Inhibitors of Proteinâ^'Protein Interactions by Fluorescence Polarizationâ€. Biochemistry, 2004, 43, 16056-16066.	2.5	243
194	Translation initiation: structures, mechanisms and evolution. Quarterly Reviews of Biophysics, 2004, 37, 197-284.	5.7	198
195	Letter to the Editor: Rapid backbone (1)H, (13)C, and (15)N assignment of the V1 domain of human PKC iota using the new program IBIS. Journal of Biomolecular NMR, 2003, 26, 373-374.	2.8	2
196	IBISa tool for automated sequential assignment of protein spectra from triple resonance experiments. Journal of Biomolecular NMR, 2003, 26, 335-344.	2.8	48
197	Structural investigations of a CYF domain covalently linked to a proline-rich peptide. Journal of Biomolecular NMR, 2003, 27, 143-149.	2.8	24
198	A sensitive and robust method for obtaining intermolecular NOEs between side chains in large protein complexes. Journal of Biomolecular NMR, 2003, 25, 235-242.	2.8	61

#	Article	IF	CITATIONS
199	Multiple-quantum magic-angle spinning spectroscopy using nonlinear sampling. Journal of Magnetic Resonance, 2003, 161, 43-55.	2.1	38
200	Broadband 13C–13C adiabatic mixing in solution optimized for high fields. Journal of Magnetic Resonance, 2003, 165, 59-79.	2.1	12
201	Ribosome Loading onto the mRNA Cap Is Driven by Conformational Coupling between eIF4G and eIF4E. Cell, 2003, 115, 739-750.	28.9	312
202	Structural basis for recruitment of CBP/p300 by hypoxia-inducible factor-1α. Proceedings of the National Academy of Sciences of the United States of America, 2002, 99, 5367-5372.	7.1	403
203	TreeDock: A Tool for Protein Docking Based on Minimizing van der Waals Energiesâ€. Journal of the American Chemical Society, 2002, 124, 1241-1250.	13.7	63
204	A Novel Approach for Characterizing Protein Ligand Complexes:Â Molecular Basis for Specificity of Small-Molecule Bcl-2 Inhibitors. Journal of the American Chemical Society, 2002, 124, 1234-1240.	13.7	123
205	Dynamic interaction of CD2 with the GYF and the SH3 domain of compartmentalized effector molecules. EMBO Journal, 2002, 21, 5985-5995.	7.8	80
206	Mechanisms Contributing to T Cell Receptor Signaling and Assembly Revealed by the Solution Structure of an Ectodomain Fragment of the CD3ϵl³ Heterodimer. Cell, 2001, 105, 913-923.	28.9	156
207	An unmediated hydrogen peroxide biosensor based on hemoglobin incorporated in a montmorillonite membrane. Analyst, The, 2001, 126, 1086-1089.	3.5	29
208	Electron-Transfer Reactivity and Enzymatic Activity of Hemoglobin in a SP Sephadex Membrane. Analytical Chemistry, 2001, 73, 2850-2854.	6.5	179
209	Incorporation of Horseradish Peroxidase in a Kieselguhr Membrane and the Application to a Mediator-free Hydrogen Peroxide Sensor Analytical Sciences, 2001, 17, 273-276.	1.6	25
210	A solubility-enhancement tag (SET) for NMR studies of poorly behaving proteins. Journal of Biomolecular NMR, 2001, 20, 11-14.	2.8	138
211	Solution structure and backbone dynamics of an omega-conotoxin precursor. Protein Science, 2001, 10, 538-550.	7.6	21
212	Identification of small-molecule inhibitors of interaction between the BH3 domain and Bcl-xL. Nature Cell Biology, 2001, 3, 173-182.	10.3	536
213	Structure and dynamics of scTCR investigated by a new NMR structural refinement methodology. Seibutsu Butsuri, 2000, 40, S26.	0.1	0
214	NMR spectroscopy: a multifaceted approach to macromolecular structure. Quarterly Reviews of Biophysics, 2000, 33, 29-65.	5.7	224
215	Recombinant decorsin: Dynamics of the RGD recognition site. Protein Science, 2000, 9, 1428-1438.	7.6	18
216	Utilization of Site-Directed Spin Labeling and High-Resolution Heteronuclear Nuclear Magnetic Resonance for Global Fold Determination of Large Proteins with Limited Nuclear Overhauser Effect Dataâ€. Biochemistry, 2000, 39, 5355-5365.	2.5	578

#	Article	IF	CITATIONS
217	Efficient Synthesis of 13C,15N-Labeled RNA Containing the Cap Structure m7GpppA. Journal of the American Chemical Society, 2000, 122, 2417-2421.	13.7	20
218	The GYF domain is a novel structural fold that is involved in lymphoid signaling through proline-rich sequences. Nature Structural Biology, 1999, 6, 656-660.	9.7	86
219	Solution structure of the catalytic domain of GCN5 histone acetyltransferase bound to coenzyme A. Nature, 1999, 400, 86-89.	27.8	96
220	Solution structure of the hRPABC14.4 subunit of human RNA polymerases. Nature Structural Biology, 1999, 6, 1039-1042.	9.7	14
221	Structure, specificity and CDR mobility of a class II restricted single-chain T-cell receptor. Nature Structural Biology, 1999, 6, 574-581.	9.7	83
222	Efficient side-chain and backbone assignment in large proteins: application to tGCN5. Journal of Biomolecular NMR, 1999, 15, 227-239.	2.8	36
223	Application of automated NOE assignment to three-dimensional structure refinement of a 28 kDa single-chain T cell receptor. , 1999, 15, 103-113.		13
224	The Crystal Structure of a T Cell Receptor in Complex with Peptide and MHC Class II. Science, 1999, 286, 1913-1921.	12.6	376
225	Structure of a Heterophilic Adhesion Complex between the Human CD2 and CD58 (LFA-3) Counterreceptors. Cell, 1999, 97, 791-803.	28.9	216
226	Identification by NMR Spectroscopy of Residues at Contact Surfaces in Large, Slowly Exchanging Macromolecular Complexes. Journal of the American Chemical Society, 1999, 121, 9903-9904.	13.7	89
227	Internal and overall motions of the translation factor eIF4E: cap binding and insertion in a CHAPS detergent micelle. Journal of Biomolecular NMR, 1998, 12, 73-88.	2.8	21
228	The interaction of elF4E with 4Eâ€BP1 is an induced fit to a completely disordered protein. Protein Science, 1998, 7, 1639-1642.	7.6	80
229	Solution Structure of the Core NFATC1/DNA Complex. Cell, 1998, 92, 687-696.	28.9	101
230	Intramolecular Masking of Nuclear Import Signal on NF-AT4 by Casein Kinase I and MEKK1. Cell, 1998, 93, 851-861.	28.9	291
231	4E Binding Proteins Inhibit the Translation Factor eIF4E without Folded Structureâ€. Biochemistry, 1998, 37, 9-15.	2.5	116
232	A Simple Method to Distinguish Intermonomer Nuclear Overhauser Effects in Homodimeric Proteins withC2Symmetry. Journal of the American Chemical Society, 1997, 119, 5958-5959.	13.7	58
233	Unusual Rel-like architecture in the DNA-binding domain of the transcription factor NFATc. Nature, 1997, 385, 172-176.	27.8	103
234	Structure of translation factor elF4E bound to m7GDP and interaction with 4E-binding protein. Nature Structural Biology, 1997, 4, 717-724.	9.7	347

#	Article	IF	CITATIONS
235	Structure and mobility of the PUT3 dimer. Nature Structural Biology, 1997, 4, 744-750.	9.7	51
236	Dimerization of the UmuD' protein in solution and its implications for regulation of SOS mutagenesis. Nature Structural Biology, 1997, 4, 979-982.	9.7	73
237	Refined solution structure of the DNA-binding domain of GAL4 and use of 3J(113Cd,1H) in structure determination. Journal of Biomolecular NMR, 1997, 10, 397-401.	2.8	17
238	The counterreceptor binding site of human CD2 exhibits an extended surface patch with multiple conformations fluctuating with millisecond to microsecond motions. Protein Science, 1997, 6, 534-542.	7.6	44
239	Refined structure of villin 14T and a detailed comparison with other actinâ€severing domains. Protein Science, 1997, 6, 1197-1209.	7.6	28
240	Quantification of Maximum-Entropy Spectrum Reconstructions. Journal of Magnetic Resonance, 1997, 125, 332-339.	2.1	62
241	Local Mobility within Villin 14T Probed via Heteronuclear Relaxation Measurements and a Reduced Spectral Density Mappingâ€. Biochemistry, 1996, 35, 1722-1732.	2.5	36
242	Use of Selective CαPulses for Improvement of HN(CA)CO–D and HN(COCA)NH–D Experiments. Journal of Magnetic Resonance Series B, 1996, 111, 194-198.	1.6	56
243	An Optimized 3D NOESY–HSQC. Journal of Magnetic Resonance Series B, 1996, 112, 200-205.	1.6	165
244	Increased Sensitivity in HNCA and HN(CO)CA Experiments by Selective CβDecoupling. Journal of Magnetic Resonance Series B, 1996, 113, 91-96.	1.6	59
245	Solution structure of the potassium channel inhibitor agitoxin 2: Caliper for probing channel geometry. Protein Science, 1995, 4, 1478-1489.	7.6	125
246	The importance of being floppy. Nature Structural and Molecular Biology, 1995, 2, 255-257.	8.2	27
247	Composition and Sequence Specific Resonance Assignments of the Heterogeneous N-Linked Glycan in the 13.6 kDa Adhesion Domain of Human Cluster of Differentiation 2 (CD2) as Determined by NMR on the Intact Glycoprotein. Biochemistry, 1995, 34, 1622-1634.	2.5	58
248	[20] Investigation of protein motions via relaxation measurements. Methods in Enzymology, 1994, 239, 563-596.	1.0	191
249	Improved resolution in triple-resonance spectra by nonlinear sampling in the constant-time domain. Journal of Biomolecular NMR, 1994, 4, 483-490.	2.8	96
250	Solution structure of villin 14T, a domain conserved among actinâ€severing proteins. Protein Science, 1994, 3, 70-81.	7.6	52
251	Thin end of the wedge. Nature Structural Biology, 1994, 1, 497-498.	9.7	5
252	Application of nonlinear sampling schemes to COSY-type spectra. Journal of Biomolecular NMR, 1993, 3, 569-76.	2.8	97

#	Article	IF	CITATIONS
253	Structure of the glycosylated adhesion domain of human T lymphocyte glycoprotein CD2. Structure, 1993, 1, 69-81.	3.3	66
254	Proton resonance assignments and secondary structure of the 13.6 kDa glycosylated adhesion domain of human CD2. Biochemistry, 1993, 32, 10995-11006.	2.5	44
255	NMR relaxation and protein mobility. Current Opinion in Structural Biology, 1993, 3, 748-754.	5.7	127
256	Design, synthesis and solution structure of a renin inhibitor Structural constraints from NOE, and homonuclear and heteronuclear coupling constants combined with distance geometry calculations. FEBS Letters, 1992, 302, 97-103.	2.8	9
257	The solution structure of eglin c based on measurements of many NOEs and coupling constants and its comparison with Xâ€ray structures. Protein Science, 1992, 1, 736-751.	7.6	411
258	Effects of DNA binding and metal substitution on the dynamics of the GAL4 DNAâ€binding domain as studied by amide proton exchange. Protein Science, 1992, 1, 1403-1412.	7.6	21
259	Solution structure of the DNA-binding domain of Cd2-GAL4 from S. cerevisiae. Nature, 1992, 356, 450-453.	27.8	134
260	A constant-time three-dimensional triple-resonance pulse scheme to correlate intraresidue 1HN, 15N, and 13C′ chemical shifts in 15Nî—,13C-labelled proteins. Journal of Magnetic Resonance, 1992, 97, 213-217.	0.5	95
261	A triple-resonance pulse scheme for selectively correlating amide1HN and15N nuclei with the1Hα proton of the preceding residue. Journal of Biomolecular NMR, 1992, 2, 389-394.	2.8	26
262	A new 3D HN(CA)HA experiment for obtaining fingerprint HN-Hα cross peaks in15N- and13C-labeled proteins. Journal of Biomolecular NMR, 1992, 2, 203-210.	2.8	83
263	NMR studies of structure and dynamics of isotope enriched proteins. Biopolymers, 1992, 32, 381-390.	2.4	12
264	Methotrexate binds in a non-productive orientation to human dihydrofolate reductase in solution, based on NMR spectroscopy. FEBS Letters, 1991, 283, 267-269.	2.8	14
265	Protein structures in solution by nuclear magnetic resonance and distance geometry. Journal of Molecular Biology, 1987, 196, 611-639.	4.2	646
266	Nuclear magnetic resonance of labile protons in the basic pancreatic trypsin inhibitor. Journal of Molecular Biology, 1979, 130, 1-18.	4.2	191
267	Kinetics of the exchange of individual amide protons in the basic pancreatic trypsin inhibitor. Journal of Molecular Biology, 1979, 130, 19-30.	4.2	117
268	Chapter 2. Low-γ Nuclei Detection Experiments for Biomolecular NMR. RSC Biomolecular Sciences, 0, , 25-52.	0.4	9